Article

Discovery Medicine 2023; 35(174): 82–94
https://doi.org/10.24976/Discov.Med.202335174.9

LncRNA *RP11-1100L3.8* Involves in the Pathogenesis of Multiple Myeloma by Regulating *NR4A1*

Youfan Feng[1,2], Xiaofang Wei[2], Yuan Fu[2], Fei Liu[2], QiaoLin Chen[2], Wenjie Zhang[2], Yangyang Zhao[2], Xiujuan Huang[2], Yang Chen[2], Qingfen Li[2], Li Zhao[3,*], Qike Zhang[2,*]

[1]The First Clinical Medical College of Lanzhou University, 730000 Lanzhou, Gansu, China
[2]Department of Hematology, Gansu Provincial Hospital, 730000 Lanzhou, Gansu, China
[3]Central Laboratory, The First Hospital of Lanzhou University, 730000 Lanzhou, Gansu, China
*Correspondence: zhaoli@lzu.edu.cn (Li Zhao); zqk05@163.com (Qike Zhang)
Published: 1 February 2023

Purpose: Although numerous studies have revealed that various long-non coding RNA (lncRNA) are implicated in multiple myeloma (MM) regulation, MM lncRNA profile and novel functional lncRNAs in MM need to be elucidated.
Methods: Herein, lncRNAs and mRNAs (messenger ribonucleic acids) patterns in MM were evaluated using RNA-sequencing (RNAseq). Differentially expressed (DE) genes were defined and a complex regulatory network based on validation and predication was shaped.
Results: LncRNA-seq data analysis identified 539 DE lncRNAs and *RP11-1100L3.8* was the most up-regulated known lncRNA. Subsequently, the upregulation and clinical *RP11-1100L3.8* utilization value was verified in an expanded cohort. Based on the results of Cis nearby-targets and co-expression analysis, 1 correlation pair *RP11-1100L3.8*-nuclear receptor subfamily 4 group A member 1 (*NR4A1*) was defined. It is worth noting that *NR4A1* is one of the top 5 significantly up-regulated DE mRNAs in MM patients. Moreover, it was found that *NR4A1* overexpression is associated with poor prognosis in MM patients, making it suitable as biomarker. Additionally, spearman correlation analysis revealed the positive association between *RP11-1100L3.8* and *NR4A1* in MM patients. Furthermore, the dominant *NR4A1* interacted genes were predicated and it was found that the genes containing *NR4A1* were remarkably enriched in phosphatidylinositol 3-kinase (PI3K)-AKT (protein kinase B) signaling pathway. In addition, *in vitro* experiment suggested that *RP11-1100L3.8* downregulation decreased *NR4A1* expression in U266 and RPMI 8226 MM cells. *RP11-1100L3.8* inhibition declined proliferation and promoted apoptosis in MM cells, which were rescued by *NR4A1* overexpression. Moreover, it was found that *RP11-1100L3.8* inhibition impeded PI3K and AKT phosphorylation and rapamycin mammalian target in MM cells, which was rescued by *NR4A1* overexpression.
Conclusions: This study identifies *RP11-1100L3.8* as a potential MM biomarker, and it may be involved in MM pathophysiology by regulating *NR4A1*-mediated PI3K-AKT signaling pathway. This study provides a novel biomarker candidate for MM therapy.

Keywords: multiple myeloma; lncRNA; biomarker; precise therapy

Introduction

Multiple myeloma (MM) is a group of incurable malignant plasma cell diseases, manifested by abnormal bone marrow plasma cells proliferation with a complex array of clinical characterizations containing compromised renal function, lytic bone lesions, anemia, hypercalcemia, and immune dysfunction. It is the second most common hematological malignancies, with approximately 176,400 new diagnosed patients and 11,7000 death cases worldwide only in 2020 [1–3]. Its traditional therapeutic method is chemotherapy or chemotherapy combined with stem cell transplantation. Recently, as the more uniform utilization of autologous stem cell transplantation and the rapid development of targeted drugs, such as proteasome inhibitors (bortezomib, carfilzomib, and ixazomib), immunomodulatory agents (lenalidomide, pomalidomide, and thalidomide), and monoclonal antibody (daratumumab and isatuximab), progression-free survival and overall survival of MM patients have improved [4,5]. However, the 10-year survival rate for MM patients remains at just 17% [6]. Thus, it is important to find new therapeutic targets to develop novel therapy strategies, that improve MM patients' prognosis.

Long-non coding RNA (lncRNA) is a type of transcribed RNA molecules longer than 200 nucleotides limiting protein coding potential due to the lack of functional open reading frames [7]. Accumulating evidences identified lncRNAs as functional tumor suppressors or oncogenes through modulating post-transcriptional modifications, regulating genes expression, and binding to mRNAs (messen-

ger ribonucleic acids) or transcription factors [8,9]. Aberrantly expressed lncRNAs link to several malignant tumors containing MM [10,11]. Hu *et al*. [12] found that lncRNA MALAT1 (metastasis-associated lung adenocarcinoma transcript 1) overexpression is associated with worse MM prognosis. Additionally, MALAT1 degradation induces DNA damage and MM cells death, making MALAT1 a promoting target for MM therapy. Xu *et al*. [13] suggested that lncRNA CCAT2 (colon cancer associated transcript 2) is upregulated in MM patients, which can be used as a candidate MM prognosis and diagnosis. Although numerous studies have revealed that various lncRNAs are implicated in MM regulation, MM lncRNA patients' profile and novel functional lncRNAs in MM need to be elucidated.

Nuclear receptor subfamily 4 group A member 1 (*NR4A1*) is a transcription factor that regulates proliferation, apoptosis, inflammation, endocrine system, and metabolism in malignant and normal cells [14–16]. Herein, this study was evaluated lncRNA profile in MM patients using RNA-sequencing (RNA-seq), and the potential functional lncRNA in MM was defined. The underlying molecular mechanism was predicated using bioinformatics analysis and validated *in vitro*.

Materials and Methods

Populations

21 patients with MM admitted to Gansu Provincial People's Hospital from July 2021 to June 2022 were selected as MM group, and another 30 matched patients with iron deficiency anemia were set as control group. Patients were diagnosed with MM according to International Myeloma Working Group 2014 [17] criteria. Exclusion criteria: MM patients with the presence of other malignancies, additional hematological malignancies and autoimmune diseases, during pregnancy or lactation, or with mental disorders and inability to cooperate with treatment. Patients' clinical characteristics were recorded, including age, gender, hemoglobin, platelets, albumin, globulin, beta-2 microglobulin, blood calcium, serum creatinine, lactate dehydrogenase, diagnosis stage DS (Durie-Salmon), ISS (international staging system), and R-ISS (revised international staging system), and bone lesions. All individuals received 4 mL of bone marrow blood for RNA-seq (MM vs. control: 5 vs. 5) and quantitative polymerase chain reaction validation (qPCR, MM vs. control: 21 vs. 30).

RNA Sequencing

Whole RNAs were obtained from bone marrow using TRIzol reagent (15596026, Invitrogen, Waltham, MA, USA). DNA digestion was performed using Dnase I. Extracted RNAs were qualified by examining A260/A280 with Nanodrop^{TM} OneCspectrophotometer (A30221, Thermo Fisher Scientific Inc., Waltham, MA, USA), and quantified using Qubit 3.0 with Qubit^{TM} RNA Broad Range Assay kit (Q10210, Life Technologies, Carlsbad, CA, USA). Two μg of total RNAs were used to preparate the stranded RNA sequencing library using Ribo-off rRNA Depletion Kit (Human/Mouse/Rat) (MRZG12324, Illumina, San Diego, CA, USA) and TruSeq Stranded mRNA Library Prep Kit (RS-122-2101, Illumina, San Diego, CA, USA) following manufacturer's instructions. The library products corresponding to 200–500 bps were enriched, quantified and finally sequenced on NovaSeq 6000 sequencer (20012850, Illumina, San Diego, CA, USA) with PE150 model.

mRNA Data Analysis

Raw sequencing data was first filtered by Trimmomatic (version 0.36, RWTH Aachen, Aachen, Germany) [18]. Low-quality reads were discarded and reads contaminated with adaptor sequences were trimmed. Then, clean reads were treated with in-house scripts to eliminate duplication bias produced by in library preparation and sequencing. Briefly, clean reads were first clustered according to the unique molecular identifier (UMI) sequences. Reads with the same UMI sequence were grouped into the same cluster, which were then compared to each other by pairwise alignment. Reads with sequence identity over 95% were extracted to a new sub-cluster. Thereafter, multiple sequence alignment was performed to obtain one consensus sequence for each sub-clusters. Deduplicated Reads were mapped to the reference genome of the human reference genome (GRCh37/HG19) using STRA (spliced transcripts alignment to a reference) software (version 2.5.3a, Cold Spring Harbor, NY, USA) [19] with default parameters. FeatureCounts (Subread-1.5.1; Bioconductor, The University of Melbourne, Parkville, VIC, Australia) was used to count the reads mapped to the exon regions of each gene, followed by calculating Reads Per Kilobase Per Million reads (RPKM). Genes differentially expressed (DE) between groups were evaluated using the edgeR package (version 3.12.1, Garvan Institute of Medical Research, Darlinghurst, NSW, Australia) [20]. *p*-value cutoff of 0.05 and Fold-change cutoff of 2 were used to consider gene expression differences statistically significant.

LncRNA Data Analysis

Mapped reads were spliced to get new transcripts by Stringtie (version 1.3.2, Johns Hopkins University, Baltimore, MD, USA). Thereafter, new fileted transcripts coding potential were predicted using CPC2 (coding potential calculator 2) (version beta, Peking University, Beijing, China), CPAT (coding potential assessment tool) (version 1.2.4, Baylor College of Medicine, Houston, TX, USA), CNCI (coding-non-coding index) (version 2, Chinese Academy of Sciences, Beijing, China) and Pfam (version 27.0, Wellcome Genome Campus, Hinxton, UK). The transcripts predicted to be non-coding in all four softwares or database were considered as novel lncRNA. Feature-

Counts (Subread-1.5.1; Bioconductor, The University of Melbourne, Parkville, VIC, Australia) was used to count the level of novel lncRNA and genome annotated known lncRNA, followed by calculating RPKM. LncRNA DE between groups were evaluated using the edgeR package (version 3.12.1, Garvan Institute of Medical Research, Darlinghurst, NSW, Australia). *p*-value cutoff of 0.05 and Fold-change cutoff of 2 were used to consider gene expression differences statistically significant.

LncRNA Targets Analysis

DE lncRNA target genes were predicted. (1) Genes within 100 kb upstream and downstream of the lncRNA locus were considered as Cis targets. (2) Co-expression of mRNA and lncRNA was analyzed by weighted correlation network analysis (WGCNA) (version 1.51, University of California, Los Angeles, CA, USA) with both, weight value and the signed R2 scale free topology model fit greater than 0.8. Finally, the intersection genes of Cis nearby-targets and co-expression were selected as lncRNA targets.

Bioinformatics Analysis

The major *NR4A1* interacted proteins were predicated using the String database (version 11.5) (https://cn.string-db.org/). Gene ontology (GO) analysis and Kyoto encyclopedia of genes and genomes (KEGG) enrichment analysis was used to determine major interacted genes, both were implemented by KOBAS (KO-based annotation system) software (version: 2.1.1, Peking University, Beijing, China) [21]. A *p*-value cutoff of 0.05 was consider statistically significant enrichment. *NR4A1* survival analysis in MM was analyzed using a previous cohort (Mulligan *et al*. [22] (2007) via the GenpmicScape database (http://www.genomicscape.com/microarray/survival.php).

Cell Culture and Treatment

U266 and RPMI 8226 MM cells were gifted from the American Type Culture Collection and found to be free from mycoplasma. All cells were incubated in RPMI-1640 medium (SH30809.01B, Hyclone, Logan, UT, USA) supplemented with 10% fetal bovine serum (16000-044, Invitrogen, Carlsbad, CA, USA) at 37 °C. 5×10^5 cells were suspended in 1.5 mL of RPMI-1640 and seeded into each well of a 6-well plate. The cells were then transfected with *RP11-1100L3.8* siRNA (si-lncRNA, sequence: 5′-GAGUCAUUCUGCAGCUCAAGC-3′ (sense), 5′-UUGAGCUGCAGAAUGACUCCA-3′ (antisense)) in combination with/without *NR4A1* agonist (OE-*NR4A1*, Cytosporone B, HY-N2148, MedChemExpress, Monmouth Junction, NJ, USA), or their negative control (NC) using Lipofectamine® 2000 (11668, Invitrogen, Carlsbad, CA, USA). After 24 h of transfection, qPCR was performed to ensure silencing was achieved.

Quantitative Polymerase Chain Reaction

Total RNA was extracted from bone marrow using Trizol (15596026, Invitrogen, Carlsbad, CA, USA) and reversetranscribed into cDNA using RevertAid Reverse Transcriptase (EP0442, Thermo Fisher Scientific Inc., Waltham, MA, USA). QPCR was performed using the THUNDERBIRD® qPCR Mix agent (15.5 μL, QPS-201, TOYOBO, Osaka, Japan) supplemented with 2.5 μM primer sequences (2.0 μL), reverse transcript product (2.0 μL) and ddH_2O (8.5 μL) under the experimental conditions of initial denaturation for 1 min at 95 °C, 40 cycles of denaturation at 95 °C for 15 s, annealing at 58 °C for 20 s, extension at 72 °C for 20 s, 65 °C for 5 s, and final extension at 72 °C for 5 min. The primer sequences were as follows: *RP11-1100L3.8*, forward (F), 5′-TACAGCAGCACTGGGCTTATTT-3′, reverse (R), 5′-ATGTGCCTTTAGTCCACGGAC-3′; *NR4A1*, F, 5′-GCTTCGGGGACTGGATTGA-3′, R, 5′-GGTGATGAGGACAAGGGCAGA-3′; *GAPDH* (internal reference), F, 5′-GGAAGCTTGTCATCAATGGAAATC-3′, R, 5′-TGATGACCCTTTTGGCTCCC-3′. Data analysis was performed using the $2^{-\Delta\Delta Ct}$ method.

Cell Counting Kit-8

RPMI 8226 and U266 MM cells proliferation was determined using the cell counting kit-8 (CCK-8) assay. 3×10^5 harvested RPMI 8226 and U266 cells were seeded in 96-well plates, and maintained at 37 °C for 24, 48, and 72 h. Thereafter, cells were maintained for 4 h with 10 μL of CCK-8 solution (CA1210, Solarbio, Beijing, China). The optical density was detected at 450 nm using an AMR-100 apparatus (Allsheng, Hangzhou, China).

Flow Cytometry

Annexin V-fluorescein isothiocyanate (FITC)/propidium iodide (PI) apoptosis assay kit (556547, BD Biosciences, Franklin Lakes, NJ, USA) was used for apoptosis evaluation. 1×10^6 MM cells were centrifuged at 400 $\times$g, 4 °C for 5 min, followed by resuspension in 200 μL of phosphate-buffered saline. Thereafter, the cells were incubated with 200 μL of binding buffer, stained for 30 min with 10 μL of Annexin V-FITC and 10 μL of PI in the dark, followed by the addition of 300 μL of binding buffer. Cells apoptosis rate were then detected using a Novocyte apparatus (ACEA Biosciences, Inc., San Diego, CA, USA).

Western Blot

Whole protein was extracted from RPMI 8226 and U266 cells using radioimmunoprecipitation assay lysis buffer (R0010, Solarbio, Beijing, China) and quantified using a bicinchoninic acid kit (PC0020, Solarbio, Beijing, China). Protein (20 μg) was separated and transferred onto polyvinylidene fluoride membranes (IPVH00010, Mil-

lipore, Burlington, MA, USA). Membranes were then blocked and cultured for 1 h with primary antibodies against *NR4A1*(A11703, Abclonal, Wuhan, China, 1:1000 diltion), b-cell lymphoma-2 (Bcl-2) (A0208, Abclonal, Wuhan, China, 1:1000 dilution), Bcl-2-associated X (Bax) (A12009, Abclonal, Wuhan, China, 1:1000 dilution), caspase 3 (9662, Cell Signaling Technology, Boston, MA, USA, 1:1000 dilution), cleaved caspase 3 (9661, Cell Signaling Technology, Boston, MA, USA, 1:1000 dilution), PI3K (phosphatidylinositol 3-kinase) (Ab191606, Abcam, Cambridge, UK, 1:1000 dilution), phosphorylated (p)-PI3K (Ab182651, Abcam, Cambridge, UK, 1:1000 dilution), AKT (protein kinase B) (Ab8805, Abcam, Cambridge, UK, 1:500 dilution), p-AKT (Ab38449, Abcam, Cambridge, UK, 1:1000 dilution), mammalian target of rapamycin (mTOR) (Ab109268, Abcam, Cambridge, UK, 1:5000 dilution), p-mTOR (Ab32028, Abcam, Cambridge, UK, 1:2000 dilution), and GAPDH (AC001, Abclonal, Wuhan, China, 1:1000 dilution). Thereafter, the membranes were incubated with goat anti-rabbit IgG (Ab6721, Abcam, Cambridge, UK, 1:20000 dilution) secondary antibody for 1 h. GAPDH served as an endogenous control.

Statistical Analysis

Mean values with standard deviation (SD), median values with range, and counts (percentage) were calculated to characterize the variables. LncRNA and mRNA levels in MM patients and control individuals were compared using the Mann-Whitney U-test for non-parametric analysis. Receiver operating characteristic (ROC) curve was performed for lncRNA and mRNA to examine its clinical utility. Correlation analysis between lncRNA and mRNA was completed using Spearman's rank correlation test. As for *in vitro* validation, all experiments were conducted in triplicates (n = 3) and the data are shown as the mean ± SD. Comparisons between two groups were performed using the one-sample *T*-test and more than two groups were performed using the one-way analysis of variance followed by Tukey's post-hoc test. Statistical significance was defined as p-value < 0.05. GraphPad Prism 7 software (GraphPad Software Inc., San Diego, CA, USA) was used for data analysis.

Results

MM Patients Overview

21 MM patients were enrolled with a mean age and a median age of 59.7 ± 6.4 years and 59.0 (range 48.0–73.0) years, respectively, 16 (76.2%) were male, and 5 (23.8%) female. Patients' baseline characteristics are shown in Table 1. Among the 21 patients, 9 (42.9%) received immunoglobulin G subtype, 5 (23.8%) received immunoglobulin A subtype, and 14 (66.7%) showed bone lesion. Mean levels of white blood cell, hemoglobin, calcium, platelet, beta-2-microglobulin, serum creatinine, lactate dehydroge-

Table 1. Baseline characteristics of MM patients.

Characteristics	MM patients (n = 21)
Age (years)	
Mean ± SD	59.7 ± 6.4
Median (range)	59.0 (48.0–73.0)
Gender	
Male, No. (%)	16 (76.2%)
Female, No. (%)	5 (23.8%)
Bone lesion, No. (%)	14 (66.7%)
Immunoglobulin subtype, No. (%)	
Immunoglobulin G	9 (42.9%)
Immunoglobulin A	5 (23.8%)
Others	7 (33.3%)
White blood cell (10^9/L)	
Mean ± SD	6.2 ± 3.2
Median (range)	4.6 (1.4–14.5)
Hemoglobin (g/L)	
Mean ± SD	99.7 ± 25.5
Median (range)	104.0 (45.0–147.0)
Calcium (mmol/L)	
Mean ± SD	2.4 ± 0.4
Median (range)	2.2 (1.9–3.5)
Platelet (10^9/L)	
Mean ± SD	147.5 ± 88.6
Median (range)	125.0 (24.0–338.0)
Beta-2-microglobulin (mg/L)	
Mean ± SD	8.6 ± 10.0
Median (range)	6.3 (1.9–49.7)
Serum creatinine (μmol/L)	
Mean ± SD	171.7 ± 212.4
Median (range)	84.6 (52.9–872.1)
Lactate dehydrogenase (U/L)	
Mean ± SD	192.0 ± 59.9
Median (range)	194.7 (61.9–319.0)
Albumin (g/L)	
Mean ± SD	32.7 ± 4.7
Median (range)	33.3 (22.0–41.0)
Globulin (g/L)	
Mean ± SD	46.6 ± 26.1
Median (range)	39.0 (17.0–108.3)
Blood urea nitrogen (mmol/L)	
Mean ± SD	11.7 ± 9.3
Median (range)	8.1 (3.1–38.4)
ISS stage, No. (%)	
I	4 (19.0%)
II	5 (23.9%)
III	12 (57.1%)
R-ISS stage, No. (%)	
I	5 (23.8%)
II	6 (28.6%)
III	8 (38.1%)
DS stage, No. (%)	
I	3 (14.3%)
II	2 (9.5%)
III	16 (76.2%)

MM, multiple myeloma; SD, standard deviation; DS, Durie-Salmon; ISS, international staging system; R-ISS, revised international staging system.

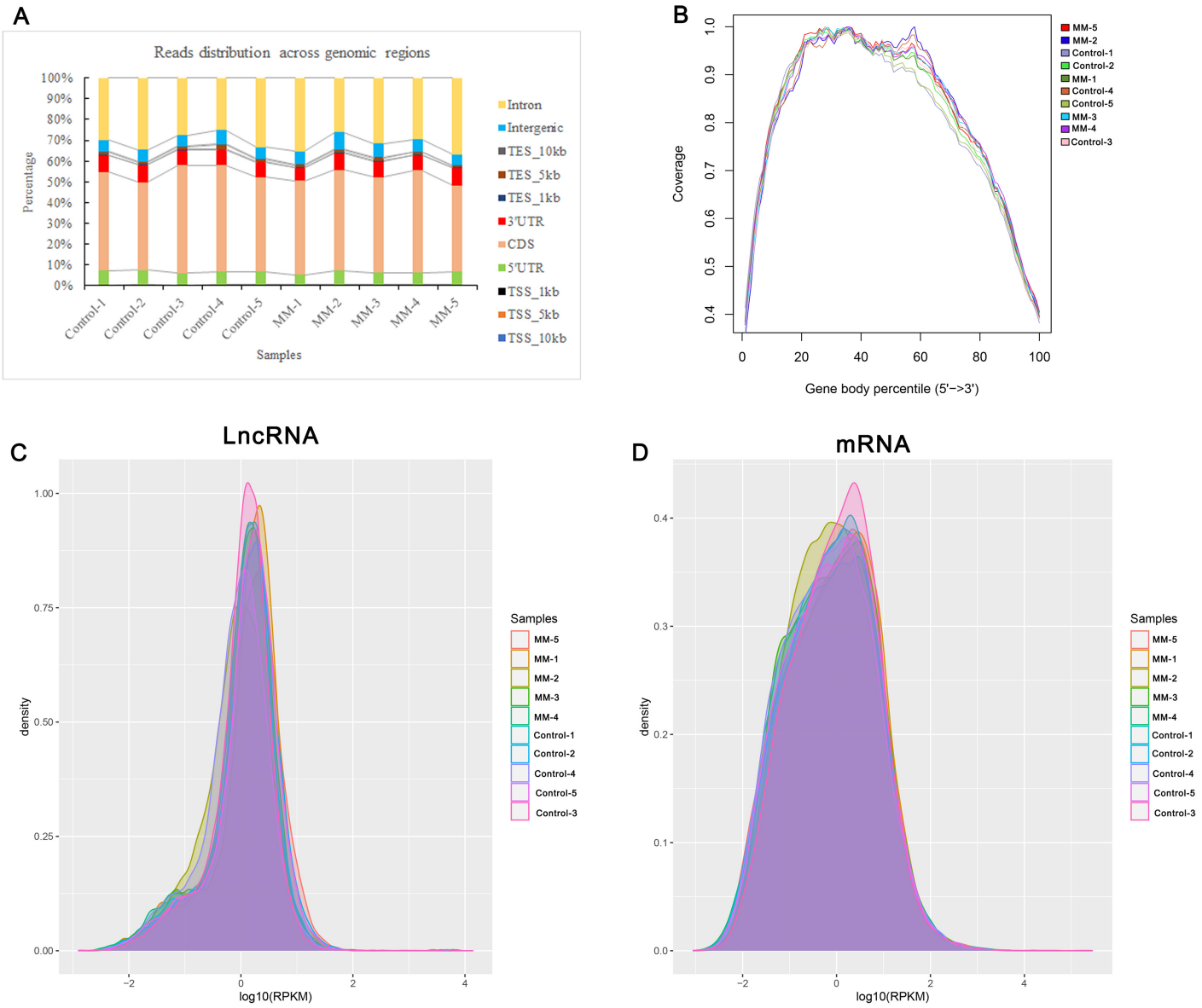

Fig. 1. RNA sequencing high quality. (A) Reads distribution across genomic regions. (B) Homogeneity distribution curve of reads across genomic regions. (C) LncRNA RPKM density distribution. (D) mRNA RPKM density distribution. RPKM, reads per kilobase per million reads.

Table 2. Sample details from RNA-seq.

Sample	Raw Data		Valid Data		Effective Rate (%)	Q20 (%)	Q30 (%)	GC (%)
	Read	Bases (G)	Read	Bases (G)				
Control 1	117891890	17.68	102106404	14.78	86.61	99.3	96.86	51.03
Control 2	109848078	16.48	95621658	13.66	87.05	99.3	96.87	51.38
Control 3	77775136	11.67	64866282	9.66	83.4	98.94	95.66	52.03
Control 4	113331822	17	96939254	14.33	85.54	99.32	96.96	55.71
Control 5	112200996	16.83	96414736	13.84	85.93	99.24	96.64	50.67
MM 1	119578904	17.94	102380714	14.74	85.62	99.25	96.7	50.68
MM 2	111631702	16.74	91277858	13.34	81.77	99.27	96.81	56.74
MM 3	105451920	15.82	88627486	12.66	84.05	99.25	96.69	51.67
MM 4	138707794	20.81	116415808	17.31	83.93	99.25	96.71	53.51
MM 5	127423180	19.11	109410116	15.54	85.86	99.33	96.98	52.12

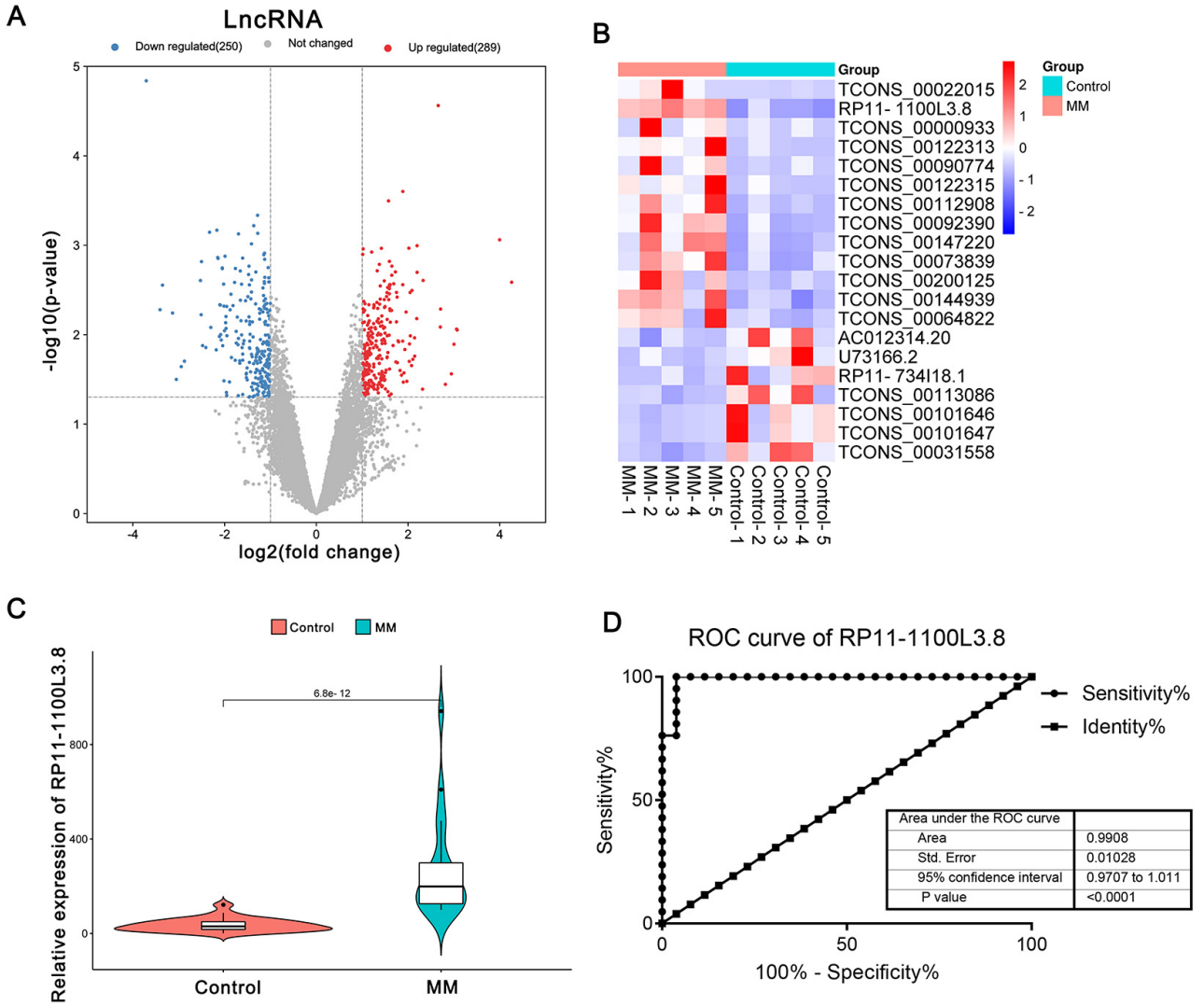

Fig. 2. LncRNA differential expression analysis. (A) Volcano plot of lncRNA expression for the MM and control groups. The vertical black dotted lines correspond to a 2.0-fold (log_2 scaled) increase and decrease, respectively. The horizontal black dotted refers to a *p*-value of 0.05 (–log10 scaled). (B) Hierarchical clustering reveals differences in lncRNA expression between the MM and control individuals. (C) *RP11-1100L3.8* expression validation experiment in MM patients. (D) *RP11-1100L3.8* receiver operating characteristic curves.

Table 3. Top 10 differentially expressed lncRNAs.

lncRNA	Log_2 (fold change)	*p*-value	Regulated
TCONS_00022015	4	0.000869	Up
RP11-1100L3.8	2.7	0.008204	Up
TCONS_00000933	2.32	0.040674	Up
TCONS_00122313	2.2	0.001011	Up
TCONS_00090774	2.14	0.017387	Up
RP11-734I18.1	–1.97	0.008506	Down
TCONS_00113086	–2.00	0.009025	Down
TCONS_00101646	–2.14	0.001405	Down
TCONS_00101647	–2.15	0.00137	Down
TCONS_00031558	–2.53	0.002481	Down

Table 4. Top 10 differentially expressed mRNAs.

mRNA	Log_2 (fold change)	*p*-value	Regulated
DUSP5	3.16	0.002107	Up
TNFAIP3	2.18	0.007335	Up
CSRNP1	2	0.043157	Up
NR4A1	1.85	0.034163	Up
TMEM176B	1.93	0.049714	Up
C9orf78	–1.67	0.002249	Down
RUNDC3A-AS1	–1.70	0.001006	Down
IFIT3	–1.78	0.031693	Down
IFIT2	–1.92	0.025217	Down
GPX1P1	-2.25	0.000219	Down

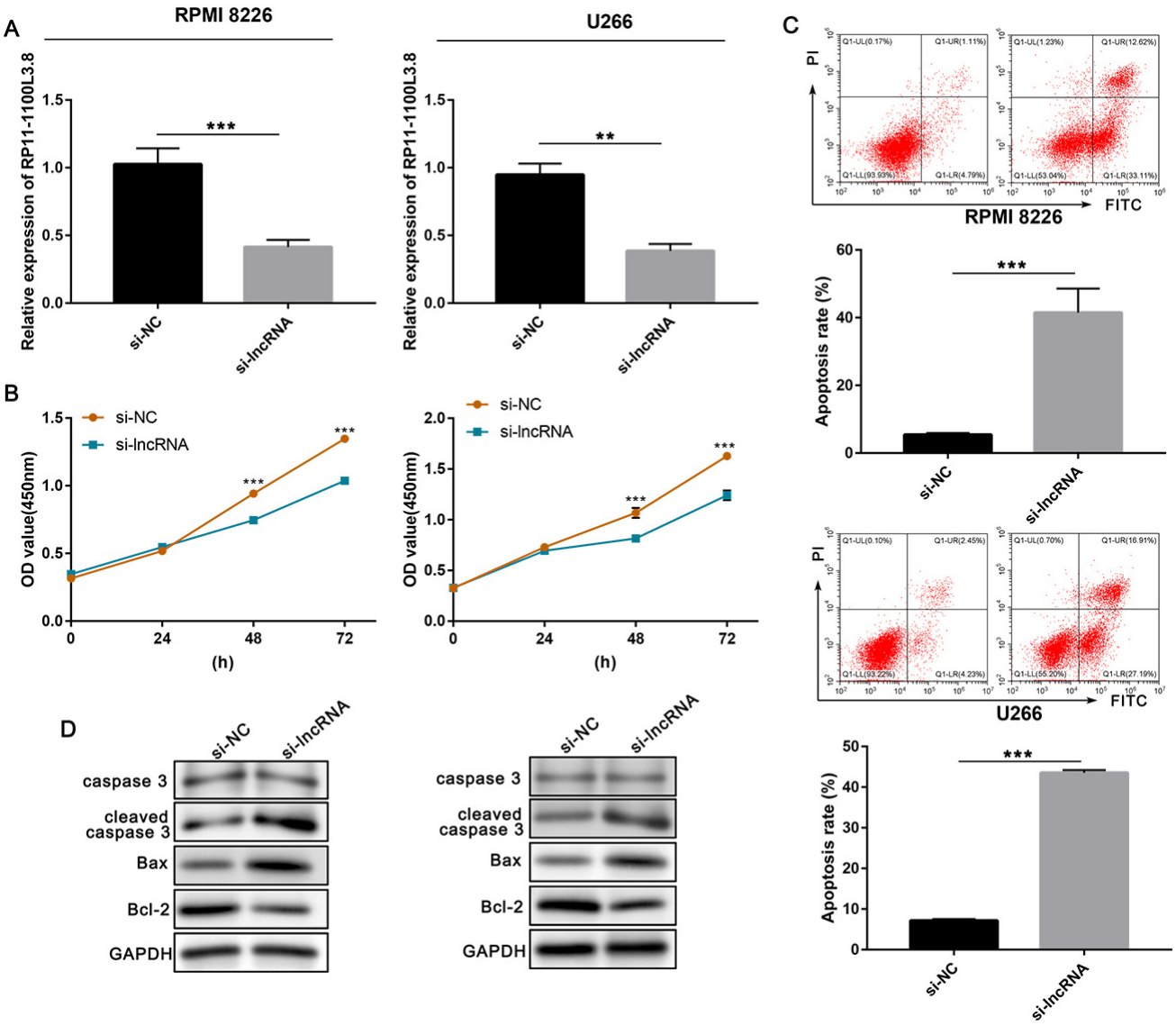

Fig. 3. LncRNA *RP11-1100L3.8* function analysis in MM cells. (A) RNA *RP11-1100L3.8* expression in RPMI 8226 and U266 MM cells. (B) Proliferation analysis of MM cells after transfection. (C) Apoptosis rate detection of MM cells after transfection. (D) Apoptosis-associated proteins expression evaluation in MM cells after transfection. $^{**}p < 0.01$, $^{***}p < 0.001$.

nase, albumin, globulin, and blood urea nitrogen were 6.2 ± 3.2 × 10^9/L, 99.7 ± 25.5 g/L, 2.4 ± 0.4 mmol/L, 147.5 ± 88.6 × 10^9/L, 8.6 ± 10.0 mg/L, 171.7 ± 212.4 μmol/L, 192.0 ± 59.9 U/L, 32.7 ± 4.7 g/L, 46.6 ± 26.1 g/L, and 11.7 ± 9.3 mmol/L, respectively. In addition, there were 4 (19.0%) patients in ISS stage I, 5 (23.9%) patients in ISS stage II, and 12 (57.1%) patients in ISS stage III. The populations in R-ISS stage I, II, III were 5 (23.8%), 6 (28.6%), and 8 (38.1%), respectively, and the populations in DS stage I, II, III there were 3 (14.3%), 2 (9.5%), and 16 (76.2%), respectively.

Differentially Expressed LncRNAs Overview

10 RNA-seq libraries were contrasted using bone marrow specimens of 5 MM patients and 5 control volunteers. It was observed that Q20 >98.94%, Q30 >95.66%, and GC content ranged from 51.03% to 56.67% (Table 2). Reads distribution across genomic regions analysis showed that the reads in each library were mainly distributed in intron and CDS (coding sequence) regions (Fig. 1A). Sequencing homogeneity analysis suggested the homogeneity of reads in each library without 5' bias or 3' bias (Fig. 1B). RPKM density distribution analysis revealed that the log10 (RPKM) of both lncRNA and mRNA was gathered at 0–1 (Fig. 1C,D). Overall, these results indicated the high quality of the data and guaranteed the reliability of follow-up analysis. Based on lncRNA-seq data analysis, it was observed that 289 lncRNAs were overexpressed and 250 lncRNAs were decreased in MM patients compared to control volunteers (Fig. 2A). Detail information about all ex-

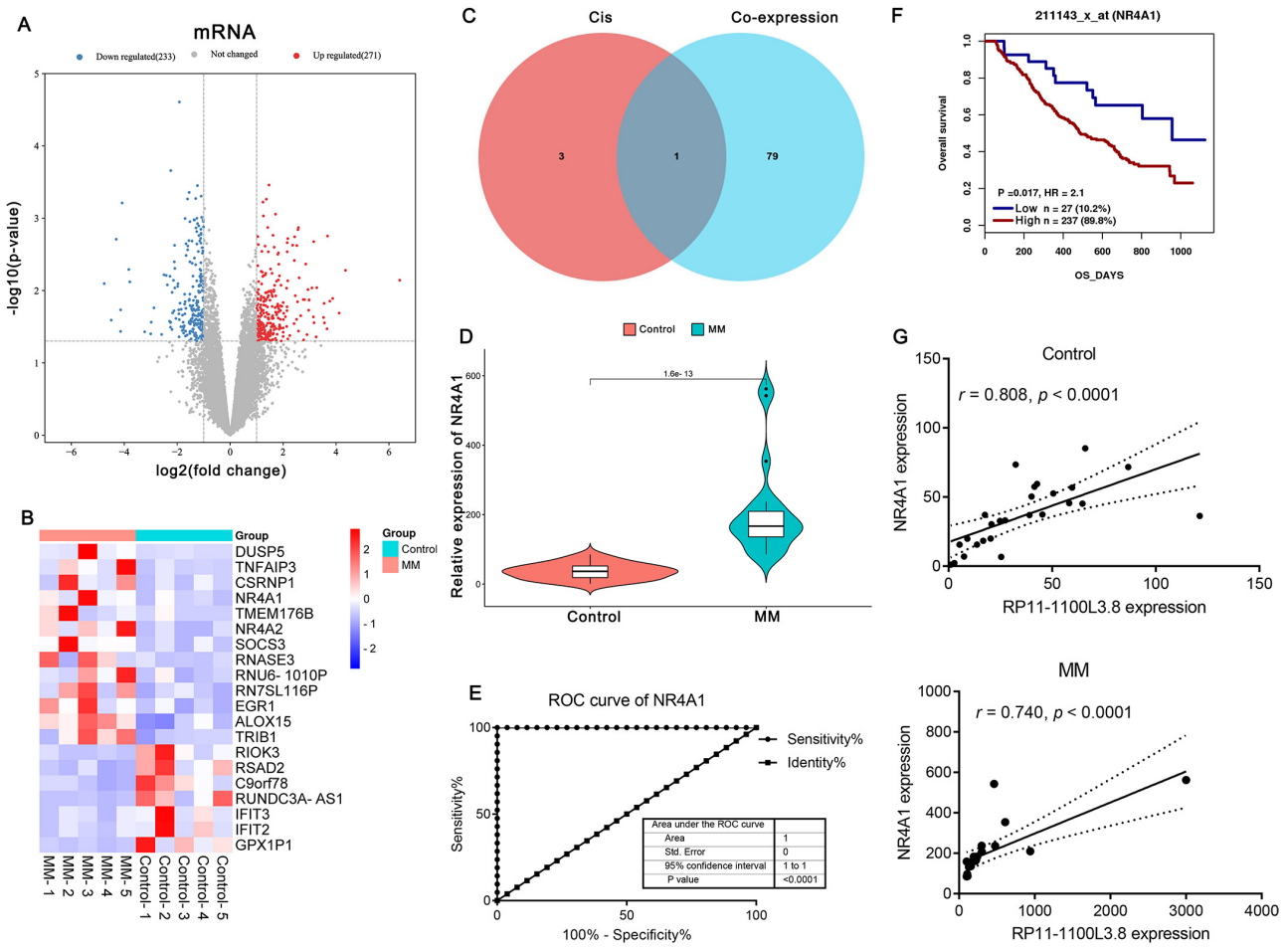

Fig. 4. mRNA differential expression analysis and expression validation of lncRNA *RP11-1100L3.8* targets. (A) mRNA expression volcano plot mRNA in the MM and control groups. The vertical black dotted lines correspond to a 2.0-fold (log_2 scaled) increase and decrease, respectively. The horizontal black dotted refers to a *p*-value of 0.05 (–log10 scaled). (B) Hierarchical clustering reveals differences in mRNA expression between the MM and control individuals. (C) *RP11-1100L3.8* Cis nearby-targets and co-expression analysis. (D) *NR4A1* expression validation experiment in MM patients. (E) *NR4A1* receiver operating characteristic curves. (F) *NR4A1* prognostic role in MM was analyzed using previous cohorts. (G) *RP11-1100L3.8* and *NR4A1* spearman correlation in both control individuals and MM patients.

pressed lncRNAs was shown in **Supplementary Table 1**. Top DE lncRNAs were selected according to the relatively high expression (RPKM) in both MM patients and control volunteers. The heatmap of the top 20 significantly DE lncRNAs in MM patients were shown in Fig. 2B. Table 3 displayed the detail information of the top 5 significantly up-regulated and downregulated DE lncRNAs, containing *RP11-1100L3.8* (upregulation) and RP11734I18.1 (down-regulation) and 8 novel lncRNAs. Since *RP11-1100L3.8* was the only one known top up-regulated DE lncRNA in MM patients, it was selected as the potential lncRNA target. QPCR was performed to validate *RP11-1100L3.8* expression in 21 MM patients and 30 control volunteers. The results validated its significantly higher expression in MM patients (Fig. 2C). ROC curve analysis showed that *RP11-1100L3.8* area under the curve (AUC) reached to 0.99 (95% confidence interval, 0.9484–1.018; $p < 0.0001$) (Fig. 2D), revealing *RP11-1100L3.8* as a valuable MM biomarker.

RP11-1100L3.8 Inhibition Suppresses Proliferation and Promotes Apoptosis of MM Cells

Furthermore, *RP11-1100L3.8* expression was inhibited in RPMI 8226 and U266 MM cells (Fig. 3A). CCK-8 assay showed the *RP11-1100L3.8* downregulation impeded proliferation of 8266 and U266 cells (Fig. 3B). Flow cytometry demonstrated that *RP11-1100L3.8* inhibition enhanced MM cells apoptosis (Fig. 3C). In addition, western blot results revealed that *RP11-1100L3.8* suppression promoted caspase cleave 3 and Bax expression, whereas inhibited Bcl-2 level (Fig. 3D and **Supplementary Fig. 1**).

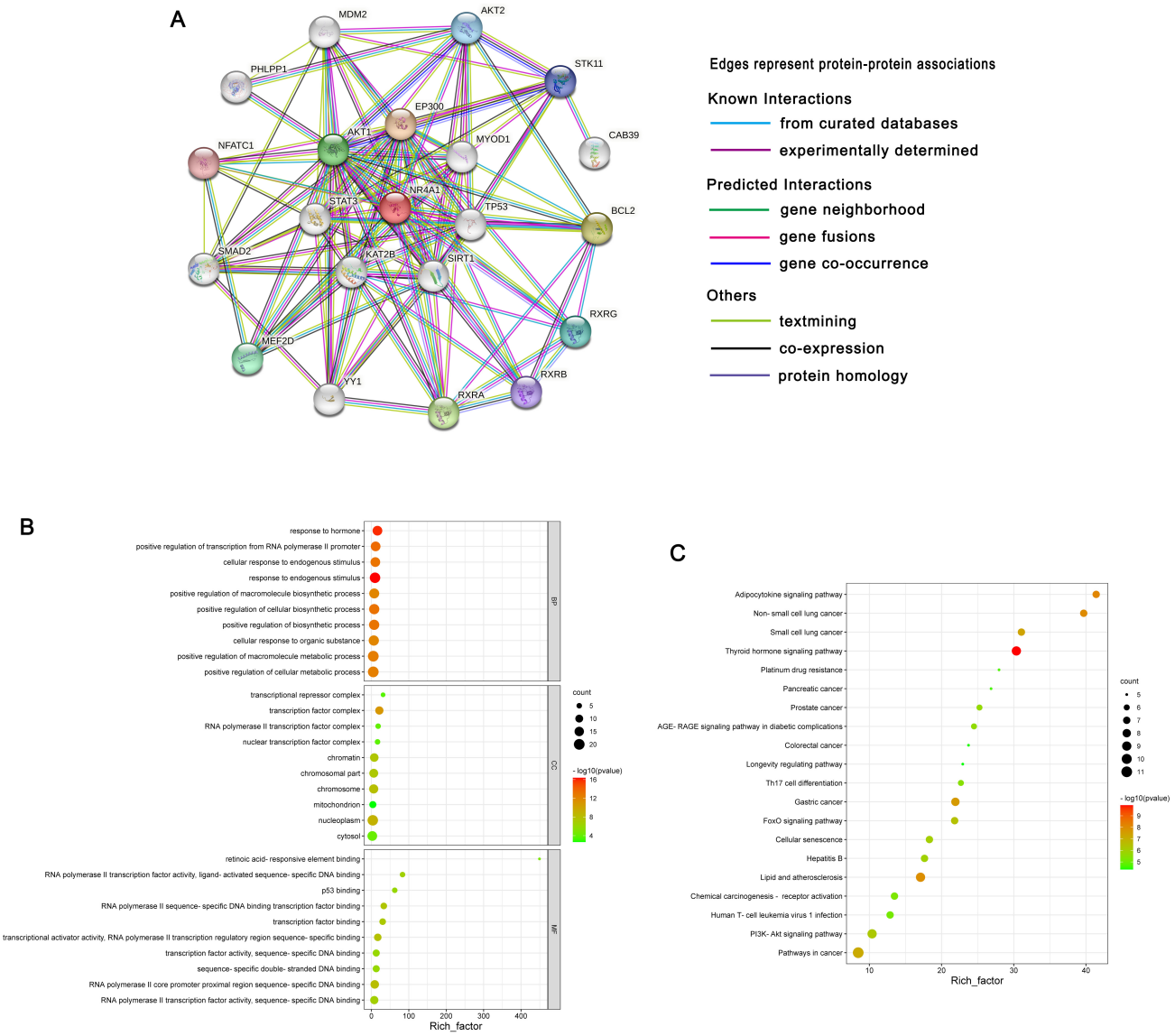

Fig. 5. *NR4A1* interacted genes functional predication. (A) *NR4A1* major interacted proteins. (B) Top 10 GO terms of biological process, cellular component, and molecular function of *NR4A1* interacted genes enrichment. (C) Top 20 KEGG pathway of *NR4A1* interacted genes enrichment.

Differentially Expressed mRNA and RP11-1100L3.8 Targets Overview

mRNA-seq data analysis revealed that 271 mRNAs were overexpressed and 233 mRNAs were decreased in MM patients compared to control volunteers (Fig. 4A). The detail information of all the expressed mRNAs was shown in **Supplementary Table 2**. Top DE mRNAs were selected according to the relatively high expression (RPKM) in both MM patients and control volunteers. Fig. 4B showed the top 20 significantly DE mRNAs in MM patients and the detail information of the top 5 significantly upregulated (*DUSP5*, *TNFAIP3*, *CSRNP1*, *NR4A1*, and *TMEM176B*) and downregulated (*C9orf78*, *RUNDC3A-AS1*, *IFIT3, IFIT2*, and *GPX1P1*) DE mRNAs were displayed in Table 4. To further explore the underlying mechanism of *RP11-1100L3.8* effect on MM patients, mRNAs transcribed within a 100 kb window up- or downstream of lncRNAs were searched. WGCNA was performed to identify *RP11-1100L3.8* targets. A total of 4 *RP11-1100L3.8* Cis nearby-targeted mRNAs pairs and 80 *RP11-1100L3.8*-mRNAs co-expression pairs were observed (Fig. 4C). Based on Cis results, nearby-targets and co-expression analysis, 1 correlation pair *RP11-1100L3.8-NR4A1* was defined. It is worth noting that *NR4A1* is one of the top 5 significantly up-regulated DE mRNAs in MM patients (Table 4). Furthermore, *NR4A1* was validated to be highly expressed in MM patients compared to that in control individuals (Fig. 4D). ROC curve analysis demonstrated that *NR4A1* AUC reached to 1.00 (95% confidence

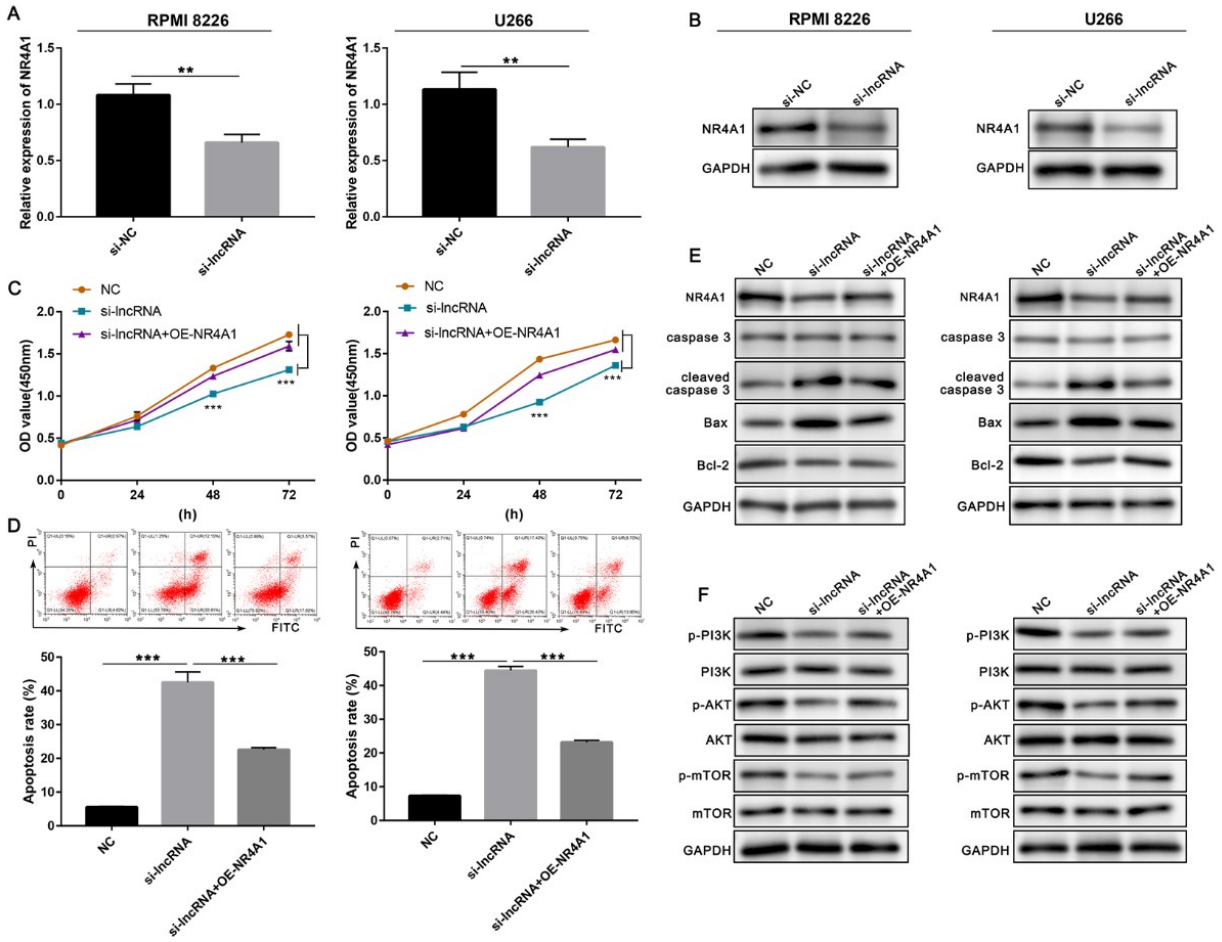

Fig. 6. *NR4A1* function analysis on lncRNA *RP11-1100L3.8* inhibited MM cells. (A) *NR4A1* mRNA and (B) protein expression in MM cells after treatment. (C) MM cells proliferation analysis after treatment. (D) MM cells apoptosis rate detection after treatment. (E) Apoptosis-associated proteins expression evaluation in MM cells after treatment. (F) PI3K-AKT-mTOR pathway activity detection in MM cells after treatment. $^{**}p < 0.01$, $^{***}p < 0.001$.

interval, 1–1; $p < 0.0001$), revealing *NR4A1* as a valuable MM biomarker (Fig. 4E). *NR4A1* prognostic role in MM was analyzed using a previous cohort [22], revealing that *NR4A1* high expression was related to worse prognosis of MM patients (Fig. 4F). In addition, spearman's rank correlation test demonstrated the positive association between *RP11-1100L3.8* and *NR4A1* in both MM patients and control individuals (Fig. 4G).

Functional Analysis of NR4A1 Interacted Genes

Furthermore, *NR4A1* feasible biological functions were evaluated. The major *NR4A1* interacted proteins were predicated using String database, including AKT1, STAT3, KAT2B, TP53, and SIRT1 among others (Fig. 5A). Functional enrichment of these interacted genes were analyzed using the GO enrichment analysis. All the GO terms containing biological process (BP), cellular component (CC), and molecular function (MF) categories were shown in **Supplementary Table 3**. BP, CC, and MF top ten terms are shown in Fig. 5B, including response to endogenous stimulus term in BP category, transcription factor complex term in CC category, and p53 binding in MF category. KEGG enrichment were performed to investigate the pathway enrichment of theses main interactional genes. All the enriched KEGG pathways are shown in **Supplementary Table 4**. The top 20 KEGG enrichment pathways are shown in Fig. 5C, containing PI3K-AKT signaling pathway and pathways in cancer. In addition, it was observed that *NR4A1* was enriched in PI3K-AKT signaling pathway.

RP11-1100L3.8 Involves in Regulating Proliferation and Apoptosis of MM Cells through Regulating NR4A1-Mediated PI3K-AKT Signaling Pathway

Further *in vitro* experiments demonstrated that *RP11-1100L3.8* inhibition reduced mRNA (Fig. 6A) and protein expression (Fig. 6B and **Supplementary Fig. 2A**) of *NR4A1* in RPMI 8226 and U266 MM cells. Proliferation inhibition induced by *RP11-1100L3.8* downregulation in MM cells was increased by *NR4A1* overexpression (Fig. 6C), whereas apoptosis promotion induced by *RP11-1100L3.8*

downregulation was impeded by *NR4A1* overexpression via reducing apoptosis rate (Fig. 6D), and regulating apoptosis-associated proteins (Fig. 6E and **Supplementary Fig. 2B**). Additionally, western blot revealed that *RP11-1100L3.8* inhibition impeded PI3K, AKT and mTOR phosphorylation in MM cells, which was rescued by *NR4A1* overexpression (Fig. 6F and **Supplementary Fig. 2C**).

Discussion

Findings of this study provide evidence demonstrating that lncRNA *RP11-1100L3.8* was significantly highly expressed in MM patients. In addition, ROC curve analysis defined lncRNA *RP11-1100L3.8* as a potential valuable biomarker for MM. Additionally, *in vitro* experiment showed that *RP11-1100L3.8* inhibition promoted RPMI 8226 and U266 MM cells apoptosis and declined proliferation. Furthermore, *RP11-1100L3.8* targets were analyzed to evaluate the underlying molecular mechanism of *RP11-1100L3.8* effect on MM patients. Based on the results of Cis nearby-targets and co-expression analysis, 1 correlation pair *RP11-1100L3.8-NR4A1* was defined. Interestingly, RNA-seq suggested that *NR4A1* is one of the top 5 significantly upregulated DE mRNAs in MM patients. Moreover, it was found that *NR4A1* overexpression is associated with poor prognosis in MM patients making it a suitable biomarker for MM. Spearman's rank correlation test showed a positive association between *RP11-1100L3.8* with *NR4A1* in both MM patients and control individuals. In addition, it was found that *RP11-1100L3.8* effect on MM cells proliferation and apoptosis were rescued by *NR4A1* overexpression. Collectively, these results identified *RP11-1100L3.8* and *NR4A1* as valuable biomarker for MM. *RP11-1100L3.8* might participate in the pathophysiology of MM by regulating *NR4A1*.

NR4A1 is a transcription factor of the steroid/thyroid hormone receptor superfamily that regulates downstream targets expression in a ligand-independent manner [23]. It controls proliferation, apoptosis, invasion, inflammation, endocrine system, and metabolism in malignant and normal cells [14–16]. It has been well investigated in variety of cancers but not in MM. *NR4A1* function in tumorigenesis is contentious. Previous evidences have shown *NR4A1* as a cancer suppressor in head and neck squamous cell carcinoma, leading to the inhibition of the head and neck squamous cell carcinoma cells proliferation [24]. Alexopoulou *et al*. [25] found the reduced expression of *NR4A1* in higher grade and metastatic breast cancer. Its re-expression resulted in the inhibition of the migration ability of breast cancer cells. In contrast, *NR4A1* was highly expressed in both cell lines and colorectal cancer tissues. Moreover, *NR4A1* knockdown suppressed proliferation, whereas induced colorectal cancer cells apoptosis [26]. Moreover, Liu *et al*. [27] found that *NR4A1* overexpression was remarkably related to a shorter 5-year overall survival in osteosarcoma patients and it may be an expectant prognostic biomarker for osteosarcoma. Jiang *et al*. [28] have also demonstrated that *NR4A1* upregulation is strongly related to survival outcomes in papillary thyroid cancer patients and its depletion notably repressed papillary thyroid cancer cells viability. Here, it was revealed that *NR4A1* was highly expressed in MM patients, associated with worse patients' prognosis. *NR4A1* controversial function in various tumors may be responsible for tumor heterogeneity and different molecular regulatory mechanisms.

Moreover, *NR4A1* possible biological functions were evaluated. GO functional enrichment analysis indicated that *NR4A1* dominant interacted genes were notably enriched in response to endogenous stimulus term, transcription factor complex term, and p53 binding term, all of which are involved in MM pathophysiology [29–31]. KEGG pathway analysis displayed that the genes containing *NR4A1* were remarkably enriched in PI3K-AKT signaling pathway. Moreover, *in vitro* analysis demonstrated that *RP11-1100L3.8* inhibition inactivated PI3K-AKT signaling pathway in MM cells, which was activated by *NR4A1* overexpression. As previously reported, *NR4A1* suppresses Dicer-let-7i-5p expression to activate AKT signaling pathway downstream under hypoxia, in turn leading to epithelial-to-mesenchymal transition (EMT) of colon cancer cells [32].

PI3K-AKT signaling pathway is known as a functional molecular pathway that controls numerous cellular process, including cell apoptosis, proliferation, metabolism, EMT, and inflammatory [33] process. Multiple myeloma growth cytokines functions by PI3K-AKT pathway, contribute as an attractive therapeutic target for MM [34]. Accumulating evidences have demonstrated the tumorigenicity of PI3K-AKT pathway activation in MM, and its blocking impedes MM pathological processes via proliferation inhibition and apoptosis promotion [35–37]. Taken together, it can be speculated that *NR4A1* is involved in MM pathophysiology by activating the PI3K-AKT signaling pathway.

Conclusions

In conclusion, the present study provided the lncRNA profile in MM patients and defined *RP11-1100L3.8* as a valuable biomarker for MM. In addition, it was suggested that *RP11-1100L3.8* might participate in MM pathophysiology by regulating *NR4A1*. Furthermore, it was revealed that *NR4A1* may be involved in MM development by activating PI3K-AKT pathway. The limitation of our current study is that the molecular regulation mechanism was only predicated using bioinformatics analysis and validated in vitro. Much more confirmatory experiments need to be performed in the follow-up study. Overall, the findings of this work propose a potential target in lncRNA-based MM therapy.

Abbreviations

LncRNA, long-non coding RNA; MM, multiple myeloma; DE, differentially expressed; PFS, progression-free survival; OS, overall survival; RNA-seq, RNA-sequencing; WGCNA, weighted correlation network analysis; GO, gene ontology; KEGG, kyoto encyclopedia of genes and genomes; CCK-8, cell counting kit-8; FITC, fluorescein isothiocyanate; PI, propidium iodide; SD, standard deviation; ROC, receiver operating characteristic.

Availability of Data and Materials

The data presented in this study are available on request from the corresponding author.

Author Contributions

YFF, XFW, LZ, and QKZ—designed this manuscript; YFF, YF, FL, QLC, WJZ, YYZ, XJH, YC, and QFL—collected and analyzed the data; YFF—performed the experiment and drafted the manuscript; XFW, LZ, and QKZ—revised the manuscript and supervised this project. All authors contributed to the article and approved the submitted version.

Ethics Approval and Consent to Participate

The study was conducted according to the guidelines of the Declaration of Helsinki, and retrospectively approved by the Ethics Committee of Gansu Provincial People's Hospital (approval number: 2022-234). All patients voluntarily participated in this study and signed informed consent.

Acknowledgment

Not applicable.

Funding

This work was supported by the Natural Science Foundation of Gansu Province (20JR5RA144) and the General Project of National Scientific Research and Cultivation Plan of Gansu Provincial Hospital (19SYPYB-13).

Conflict of Interest

The authors declare no conflict of interest.

Supplementary Material

Supplementary material associated with this article can be found, in the online version, at https://doi.org/10.24976/Discov.Med.202335174.9.

References

[1] Al-Yafeai Z, Ghoweba M, Ananthaneni A, Abduljabar H, Aziz D. Cardiovascular complications of modern multiple myeloma therapy: A pharmacovigilance study. *Br J Clin Pharmacol*. 2023;89(2):641–648. doi: 10.1111/bcp.15499

[2] Neuse CJ, Lomas OC, Schliemann C, *et al*. Genome instability in multiple myeloma. *Leukemia*. 2020;34(11):2887–2897. doi: 10.1038/s41375-020-0921-y

[3] Sung H, Ferlay J, Siegel RL, *et al*. Global Cancer Statistics 2020: GLOBOCAN Estimates of Incidence and Mortality Worldwide for 36 Cancers in 185 Countries. *CA Cancer J Clin*. 2021;71(3):209–249. doi: 10.3322/caac.21660

[4] Goel U, Usmani S, Kumar S. Current approaches to management of newly diagnosed multiple myeloma. *Am J Hematol*. 2022;97 Suppl 1:S3–S25. doi: 10.1002/ajh.26512

[5] Goldman-Mazur S, Kumar SK. Current approaches to management of high-risk multiple myeloma. *Am J Hematol*. 2021;96(7):854–871. doi: 10.1002/ajh.26161

[6] Wallington-Beddoe CT, Mynott RL. Prognostic and predictive biomarker developments in multiple myeloma. J Hematol Oncol. 2021;14(1):151. doi: 10.1186/s13045-021-01162-7

[7] Quinn JJ, Chang HY. Unique features of long non-coding RNA biogeneis and function. *Nat Rev Genet*. 2016;17(1):47–62. doi: 10.1038/nrg.2015.10

[8] Sun C, Huang L, Li Z, *et al*. Long non-coding RNA MIAT in development and disease: a new player in an old game. *J Biomed Sci*. 2018;25(1):23. doi: 10.1186/s12929-018-0427-3

[9] Zhou L, Zhu Y, Sun D, Zhang Q. Emerging Roles of Long non-coding RNAs in The Tumor Microenvironment. *Int J Biol Sci*. 2020;16(12):2094–2103. doi: 10.7150/ijbs.44420

[10] Lavorgna G, Vago R, Sarmini M, Montorsi F, Salonia A, Bellone M. Long non-coding RNAs as novel therapeutic targets in cancer. *Pharmacol Res*. 2016;110:131–138. doi: 10.1016/j.phrs.2016.05.018

[11] Carrasco-Leon A, Ezponda T, Meydan C, *et al*. Characterization of complete lncRNAs transcriptome reveals the functional and clinical impact of lncRNAs in multiple myeloma. *Leukemia*. 2021;35(5):1438–1450. doi: 10.1038/s41375-021-01147-y

[12] Hu Y, Lin J, Fang H, *et al*. Targeting the MALAT1/PARP1/LIG3 complex induces DNA damage and apoptosis in multiple myeloma. *Leukemia*. 2018;32(10):2250–2262. doi: 10.1038/s41375-018-0104-2

[13] Xu H, Yin Q, Shen X, Ju S. Long non-coding RNA CCAT2 as a potential serum biomarker for diagnosis and prognosis of multiple myeloma. *Ann Hematol*. 2020;99(9):2159–2171. doi: 10.1007/s00277-020-04161-9

[14] Campos-Melo D, Galleguillos D, Sanchez N, Gysling K, Andres ME. Nur transcription factors in stress and addiction. *Front Mol Neurosci*. 2013;6:44. doi: 10.3389/fnmol.2013.00044

[15] Safe S, Jin UH, Morpurgo B, Abudayyeh A, Singh M, Tjalkens RB. Nuclear receptor 4A (NR4A) family—orphans no more. *J Steroid Biochem Mol Biol*. 2016;157:48–60. doi: 10.1016/j.jsbmb.2015.04.016

[16] Zhou F, Drabsch Y, Dekker TJ , *et al*. Nuclear receptor NR4A1 promotes breast cancer invasion and metastasis by activating TGF-beta signalling. *Nat Commun*. 2014;5:3388. doi: 10.1038/ncomms4388

[17] [2014 International Myeloma Working Group updated criteria for the diagnosis of multiple myeloma]. *Nihon Rinsho*. 2016;74 Suppl 5: 264–268. Japanese

[18] Bolger AM, Lohse M, Usadel B. Trimmomatic: a flexible trimmer for Illumina sequence data. *Bioinformatics*. 2014;30(15):2114–2120. doi: 10.1093/bioinformatics/btu170

[19] Dobin A, Davis CA, Schlesinger F, *et al*. STAR: ultrafast universal RNA-seq aligner. *Bioinformatics*. 2013;29(1):15–21. doi:

10.1093/bioinformatics/bts635
[20] Robinson MD, McCarthy DJ, Smyth GK. edgeR: a Bioconductor package for differential expression analysis of digital gene expression data. *Bioinformatics*. 2010;26(1):139–140. doi: 10.1093/bioinformatics/btp616
[21] Wu J, Mao X, Cai T, Luo J, Wei L. KOBAS server: a web-based platform for automated annotation and pathway identification. *Nucleic Acids Res*. 2006;34(Web Server issue):W720–W724. doi: 10.1093/nar/gkl167
[22] Mulligan G, Mitsiades C, Bryant B, *et al*. Gene expression profiling and correlation with outcome in clinical trials of the proteasome inhibitor bortezomib. *Blood*. 2007;109(8):3177–3188. doi: 10.1182/blood-2006-09-044974
[23] Kurakula K, Koenis DS, van Tiel CM, de Vries CJ. NR4A nuclear receptors are orphans but not lonesome. *Biochim Biophys Acta*. 2014;1843(11):2543–2555. doi: 10.1016/j.bbamcr.2014.06.010
[24] Wang Y, Ren X, Li W, *et al*. SPDEF suppresses head and neck squamous cell carcinoma progression by transcriptionally activating NR4A1. *Int J Oral Sci*. 2021;13(1):33. doi: 10.1038/s41368-021-00138-0
[25] Alexopoulou AN, Leao M, Caballero OL, *et al*. Dissecting the transcriptional networks underlying breast cancer: NR4A1 reduces the migration of normal and breast cancer cell lines. *Breast Cancer Res*. 2010;12(4):R51. doi: 10.1186/bcr2610
[26] Liu Z, Gu Y, Cheng X, *et al*. Upregulation lnc-NEAT1 contributes to colorectal cancer progression through sponging miR-486-5p and activating NR4A1/Wnt/beta-catenin pathway. *Cancer Biomark*. 2021;30(3):309–319. doi: 10.3233/CBM-201733
[27] Liu W, Hao Y, Tian X, Jiang J, Qiu Q. The Role of NR4A1 in the Pathophysiology of Osteosarcoma: A Comprehensive Bioinformatics Analysis of the Single-Cell RNA Sequencing Dataset. *Front Oncol*. 2022;12:879288. doi: 10.3389/fonc.2022.879288
[28] Jiang C, He J, Xu S, Wang Q, Cheng J. NR4A1 promotes LEF1 expression in the pathogenesis of papillary thyroid cancer. *Cell Death Discov*. 2022;8(1):46. doi: 10.1038/s41420-022-00843-7
[29] Wen Z, Rajagopalan A, Flietner ED, *et al*. Expression of NrasQ61R and MYC transgene in germinal center B cells induces a highly malignant multiple myeloma in mice. *Blood*. 2021;137(1):61–74. doi: 10.1182/blood.2020007156
[30] Li S, Vallet S, Sacco A, Roccaro A, Lentzsch S, Podar K. Targeting transcription factors in multiple myeloma: evolving therapeutic strategies. *Expert Opin Investig Drugs*. 2019;28(5):445–462. doi: 10.1080/13543784.2019.1605354
[31] Petrusca DN, Toscani D, Wang FM, *et al*. Growth factor independence 1 expression in myeloma cells enhances their growth, survival, and osteoclastogenesis. *J Hematol Oncol*. 2018;11(1):123. doi: 10.1186/s13045-018-0666-5
[32] Shi Z, To SKY, Zhang S, *et al*. Hypoxia-induced Nur77 activates PI3K/Akt signaling via suppression of Dicer/let-7i-5p to induce epithelial-to-mesenchymal transition. *Theranostics*. 2021;11(7):3376–3391. doi: 10.7150/thno.52190
[33] Li L, Zhu H, Li X, Ke Y, Yang S, Cheng Q. Long noncoding RNA HAGLROS facilitates the malignant phenotypes of NSCLC cells via repressing miR-100 and up-regulating SMARCA5. *Biomed J*. 2021;44(6 Suppl 2):S305–S315. doi: 10.1016/j.bj.2020.12.008
[34] Hu J, Hu WX. Targeting signaling pathways in multiple myeloma: Pathogenesis and implication for treatments. *Cancer Lett*. 2018;414:214–221. doi: 10.1016/j.canlet.2017.11.020
[35] Liu S, Zhang Y, Huang C, Lin S. miR-215-5p is an anticancer gene in multiple myeloma by targeting RUNX1 and deactivating the PI3K/AKT/mTOR pathway. *J Cell Biochem*. 2020;121(2):1475–1490. doi: 10.1002/jcb.29383
[36] Zi Y, Zhang Y, Wu Y, Zhang L, Yang R, Huang Y. Down-regulation of microRNA-25-3p inhibits the proliferation and promotes the apoptosis of multiple myeloma cells via targeting the PTEN/PI3K/AKT signaling pathway. *Int J Mol Med*. 2021;47(3). doi: 10.3892/ijmm.2020.4841
[37] Chatterjee M, Andrulis M, Stuhmer T, *et al*. The PI3K/Akt signaling pathway regulates the expression of Hsp70, which critically contributes to Hsp90-chaperone function and tumor cell survival in multiple myeloma. *Haematologica*. 2013;98(7):1132–1141. doi: 10.3324/haematol.2012.066175